

High Efficiency DC-DC Converter with two Input Power Sources using Fuzzy Logic Controller

MuthuKumaran.M

Pg Student/Department of EEE
Sethu Institute Of
Technology,Kariapatti,Virudhunagar

RadhaLakshmi.K

Assistant Professor/Department of EEE
Sethu Institute Of
Technology,Kariapatti,Virudhunagar

Abstract—The aim of this study is to develop a high efficiency converter with two input power sources for a distributed power generation mechanism. The proposed converter can boost the varied voltages of different power sources in the sense of hybrid power supply to a stable power output dc voltage for the load demand. An auxiliary circuit in the proposed converter is employed for achieving turn-On zero -voltage switching (ZVS) of all the switches. According to various situations, the operation states of the proposed converter can be divided into two states including a single power supply and a dual power supply. In the dual power supply state, the input circuits connected in series together with the designed pulse width modulation can greatly reduced the conduction losses of the switches. An effective improvement in efficiency can be achieved by using a closed loop “Fuzzy Logic Controller”(FLC) in the proposed topology.

Index terms -DC-DCconverter,hybridpowersupply,high-efficiencypowerconversion,zero -voltage switching(ZVS).

I. INTRODUCTION

In order to protect the natural environment on the earth, the development of clean energy[1]-[3] without pollution has the major representative role in the last decade. By accompanying the permission of Kyoto Protocol, clean energies, such as fuel cell (FC), photovoltaic (PV), wind energy, etc., have been rapidly promoted. Due to the electric characteristics of clean energies, the generated power is critically affected by the climate or has slow transient responses, and the output voltage is easily influenced by load variations[4]. Thus, a storage element is necessary to ensure proper operation of clean energies.

Batteries or supercapacitors are usually taken as storage mechanisms for smoothing output power, start-up transition, and various load conditions[5].The corresponding installed capacity of clean energies can be further reduced to save the cost of system purchasing and power supply. For these reasons, hybrid power conversion systems (PCS) have become one of interesting research topics for engineers and scientists at present. Based on power electronics technique, the diversely developed power conditioners including dc–dc converters and dc–ac inverters are essential components for clean-energy applications.

Generally, one power source needs a dc–dc converter either for rising the input voltage to a certain band or for regulating the input voltage to a constant dc-bus voltage[6]-

[8].However, conventional converter structures have the disadvantages of large size, complex topology, and expensive cost. In order to simplify circuit topology, improve system performance, and reduce manufacturing cost, multi-input converters have received more attentions in recent years [9]-[18].

Liu and Chen [9]proposed a general approach for developing multi-input converters. By analyzing the topologies of converters, the method for synthesizing multi-input converters was inspired by adding an extra pulsating voltage or a current source to a converter with an appropriate connection.

Waiet al. presented multi-input converters with high step-up ratios, and the goal of high-efficiency conversion was obtained. However, these topologies are not economic for the non isolated applications because of the complexity with numbers of electrical components.

Tao et al.[13] and Matsuo et al[14] utilized multi winding-type transformers to accomplish the power conversion target of multi-input sources. Although these topologies were designed based on time-sharing concept, the complexity of driving circuits will be increased by the control techniques.

Marchesoni and Vacca[15] investigated a newly designed converter with the series-connected input circuits to achieve the goal of multiple input power sources. The installation cost of the converter with few components was certainly reduced. The feature of[15] is that the conduction losses of switches can be greatly reduced, especially in the dual power supply state. Unfortunately, the hard-switching problem and the huge reverse-recovery current within the output diode degrade the conversion efficiency as a traditional boost converter[6] .

Kwasinski [16]discussed the evolution of multiple input converters from their respective single-input versions. Based on several assumptions, restrictions, and conditions, these analyses indicate some feasible and unfeasible frameworks for multiple input development. Li et al.[17] investigated a set of basic rules for generating multiple-input

auxiliary capacitor. Therefore, the switch current i_{S1} is negative. Besides, the auxiliary inductor current i_{La} linearly increases, and the slope is dependent on the auxiliary inductor voltage v_{La} , which is equal to $V_a - V_o$. Continuously, the primary auxiliary diode $Da1$ is conducted.

Mode 3 [t2 –t3]: At t_2 , the auxiliary switch S_a is turned ON with ZVS. After the auxiliary inductor current i_{La} increases to be larger than the secondary inductor current i_{L2} , the auxiliary switch current i_{Sa} becomes positive. The discharging current from the auxiliary capacitor together with the secondary inductor current i_{L2} releases the stored energy to the output voltage V_o . During modes 2 to 3 ($t = t_1 - t_3$), the time interval can be written as $(d+d_2)TS$. The auxiliary inductor current i_{La} and the secondary inductor current i_{L2} can be expressed as

$$i_{La}(t) = (V_a - V_o)(t - t_1) / L_a \quad (1)$$

Mode 4 [t3 –t4]: At t_3 , the strain. Besides, the auxiliary inductor voltage v_{La} is equal to $-V_o$, and the current i_{La} linearly decreases. The energy stored in the auxiliary inductor L_a starts to discharge into the output voltage V_o as freewheeling.

Mode 5 [t4 –t5]: At t_5 , the switch S_2 is turned ON with ZVS upon the condition that the auxiliary inductor current i_{La} is still larger than the secondary inductor current i_{L2} . The auxiliary inductor current i_{La} continuously decreases with the slope $-V_o/L_a$. After the current i_{La} is smaller than the secondary inductor current i_{L2} , the switch current i_{S2} is positive. By the same way, the switch current i_{S1} becomes positive as well as i_{S2} . During modes 4 to 5 ($t = t_3 - t_5$), the time interval can be written as $(d+d_{cm2})TS$. The auxiliary inductor current i_{La} and the secondary inductor current i_{L2} can be expressed as

$$i_{La}(t) = [(V_a - V_o)(d+d_2)TS - V_o(t - t_3)] / L_a \quad (2)$$

$$i_{L2}(t) = (I_{L2} - 0.5\Delta i_{L2}) + V_2(t - t_3) / L_2 \quad (3)$$

Mode 6 [t5 –t6]: At t_5 , the auxiliary inductor current i_{La} is equal to zero. Substituting $i_{La}(t_5) = 0$ into (17), the relation between the voltages V_a and V_o can be derived as In this mode, the parasitic capacitor of the primary diode $Da1$ is charged by the output voltage V_o with a small reverse-recovery current.

Mode 7 [t6 –t7]: At t_6 , the diode voltage v_{Da1} is rising to the output voltage V_o , the secondary auxiliary diode $Da2$ is conducted for receiving the auxiliary inductor current i_{La} to charge the auxiliary capacitor.

Mode 8 [t7 –t8]: At t_7 , the auxiliary inductor current i_{La} returns to zero. The switches S_1 and S_2 are continuously conducted. Mode 8 is similar to mode 1.

Mode 9 [t8 –t9]: At t_8 , the switch S_1 is turned OFF, the switch voltage v_{S1} is rising to the auxiliary capacitor voltage V_a , and the auxiliary switch voltage v_{Sa} is decreasing to zero. The body diode of the auxiliary switch S_a is conducted for carrying the primary inductor current i_{L1} to charge the auxiliary capacitor. The auxiliary inductor current i_{La} linearly increases with the slope $(V_a - V_o) / L_a$. Continuously, the primary auxiliary diode $Da1$ is conducted.

Mode 10 [t9 –t10]: At t_9 , the auxiliary switch S_a is turned ON with ZVS. After the auxiliary inductor current i_{La} increases to be larger than the primary inductor current i_{L1} , the auxiliary switch current i_{Sa} becomes positive. The discharging current from the auxiliary capacitor together with the primary inductor current i_{L1} releases.

Mode 11 [t10 –t11]: At t_{10} , the auxiliary switch S_a is turned OFF. Because the auxiliary inductor current i_{La} is greater than the primary inductor current i_{L1} , the parasitic capacitor of the stored energy to the output voltage V_o . auxiliary switch S_a is charged by the auxiliary inductor current i_{La} . At the same time, the energy stored in the parasitic capacitor of the switch S_1 will release to the output voltage V_o via the inductor current i_{La} .

Mode 12 [t11 –t12]: At t_{11} , the switch S_1 is turned ON with ZVS. The auxiliary inductor current i_{La} continuously decreases with the slope $-V_o/L_a$. After the current i_{La} is smaller than the primary inductor current i_{L1} , the switch current i_{S1} is positive. By the same way, the switch current i_{S2} becomes positive as well as i_{S1} . During modes 11 to 12 ($t = t_{10} \sim t_{12}$), the time interval can be written as $(d+d_{cm1})TS$. The auxiliary inductor current i_{La} and the primary inductor current i_{L1} can be expressed as

$$i_{La}(t) = [(V_a - V_o)(d+d_1)TS - V_o(t - t_{10})] / L_a \quad (4)$$

$$i_{L1}(t) = (I_{L1} - 0.5\Delta i_{L1}) + V_1(t - t_{10}) / L_1 \quad (5)$$

Auxiliary switch S_a is turned OFF. Because the auxiliary inductor current i_{La} is greater than the secondary inductor current i_{L2} , the parasitic capacitor of the auxiliary switch S_a is charged by the auxiliary inductor current i_{La} , and the auxiliary switch voltage V_{Sa} rises. At the same time, the energy stored in the parasitic capacitor of the switch S_2 will release to the output voltage V_o via the inductor current i_{La} , and the switch voltage v_{S2} decreases. The switch current i_{Sa} falls down to zero and the switch voltage V_{Sa} rises to the auxiliary capacitor voltage V_a .

Mode 13 [t12 –t13]: At t_{12} , the auxiliary inductor current i_{La} is equal to zero. Substituting $i_{La}(t_{12}) = 0$, the relation between the voltages V_a and V_o can be derived as

$$(V_a - V_o)(dd + da1) = V_o (dd + ddc1) \quad (6)$$

Mode 13 is similar to mode 6 as well as the reverse-recovery time of the primary auxiliary diode Da1 .

Mode 14 [t13-t14]: At t13, the diode voltage vDa1 is rising to the output voltage Vo , and the secondary auxiliary diode Da2is conducted for receiving the auxiliary inductor current iLato charge the auxiliary capacitor.

III . CLOSED LOOP CONTROL- FLC

In Closed loop, Fuzzy logic starts with the concept of a fuzzy set. A fuzzy set is a set without a crisp, clearly defined boundary. It can contain elements with only a partial degree of membership.

A membership function is a curve that defines how each point in the input space is mapped to a membership value (or degree of membership) between 0 and 1. The input space is sometimes referred to as the universe of discourse. A fuzzy set admits the possibility of partial membership in it. The degree an object belongs to a fuzzy set is denoted by a membership value between 0 and 1.

A membership function associated with a given fuzzy set maps an input value to its appropriate membership. Fuzzy systems theory enables us to utilize qualitative, linguistic information about a system to construct a mathematical model for it. For many real-life systems, which are highly complex and inherently nonlinear, conventional approaches to modeling are not easy to apply, whereas the fuzzy approach might be a very helpful alternative.

Fuzzy models can be seen as rule-based systems suitable for formalizing the knowledge of experts. Fuzzy control is easy to learn and easy to apply, since it is close to human intuition. Functions are provided for many common methods, including fuzzy clustering and adaptive neuro fuzzy learning.

FLC have some advantages compared to other classical controller such as simplicity of control, low cost and the possibility to design without knowing the exact mathematical model of the process Fuzzy logic is a more intuitive approach without the far-reaching complexity. Structure of a fuzzy logic controller consists of: input, fuzzification.

Rule base, defuzzification, output. There are specific components characteristic of a fuzzy controller to support a design procedure. It shows the controller between the input and output. The inputs are most often hard or crisp measurement from some measuring equipment is converted into fuzzy values for each input fuzzy set with the fuzzification block.

The first block inside the controller is fuzzification which converts each piece of input data to degrees of membership by a lookup in one or several membership functions. The fuzzification block matches the input data with the conditions of the rules to determine.

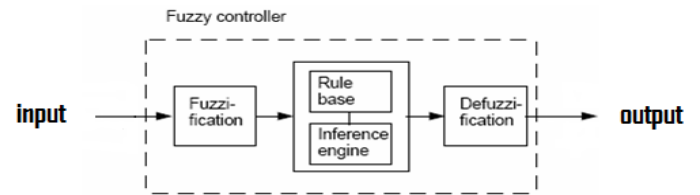


Figure 2. Structure of Fuzzy logic control

The computer is able to execute the rules and compute a control signal depending on the measured inputs error (e) and change in error.(dE). In a rule based controller the control strategy is stored in a more or less natural language. A rule base controller is easy to understand and easy to maintain for a non- specialist end user and an equivalent controller could be implemented using conventional techniques

Defuzzification is when all the actions that have been activated are combined and converted into a single non-fuzzy output signal which is the control signal of the system. The output levels are depending on the rules that the systems have and the positions depending on the non-linearity's existing to the systems.

To achieve the result, develop the control curve of the system representing the I/O relation of the systems and based on the information; define the output degree of the membership function with the aim to minimize the effect of the non-linearity and the output is output gain that can be tuned and also become as an integrator .The output crisp value can be calculated by the centre of gravity or the weighted average.

In our proposed system, by dynamically calculating the nodes trust vector values, the source node can be able to select the more trusted routes rather than selecting the shorter routes. Our system marks and isolates the malicious nodes from participating in the network. So the potential damage caused by the malicious is reduced.

Let $\{Tv_1, Tv2, \dots\}$ be the initial trust vectors of the nodes $\{n_1, n2, \dots\}$ along the route R1 from a source S to the destination D.

Since the node does not have any information about the reliability of its neighbors in the beginning, nodes can neither be fully trusted nor be fully distrusted. When a source S want to establish a route to the destination D, it send route request (RREQ) packets .

When the destination D receives the accumulated RREQ message, it measures the number of packets received Prec. Then it constructs a route on Prec with the key shared by the sender and the destination. The RREP contains the source and destination ids, the route of Prec, the accumulated route from the RREQ, which are digitally signed by the destination. The RREP is sent towards the source on the reverse route R1.

The intermediate node then verifies the digital signature of the destination node stored in the RREP packet, is valid. If the verification fails, then the RREP packet is dropped. Otherwise, it is signed by the intermediate node and forwarded to the next node in the reverse route.

When the source S receives the RREP packet, it first verifies that the first id of the route stored by the RREP is its neighbor. If it is true, then it verifies all the digital signatures of the intermediate nodes, in the RREP packet. The digital signature includes recommendation about the neighbor node and probability that data packet received successfully. If all these verifications are successful, then the trust counter values of the nodes are incremented as

$$Tv_i = Tv_i + \alpha_1 \tag{1}$$

If the verification is failed, then

$$Tv_i = Tv_i - \alpha_1 \tag{2}$$

Where α_1 is the step value, which can be assigned a small fractional value during simulations. After this verification stage, the source S check the digital signature values DS of the nodes n_i .

Digital Signature includes recommendation about the neighbor node and probability that data packet received successfully.

Evaluating the recommendation is given by R_B^A which is node A's evaluation to node B by collecting recommendations

$$R_B^A = \frac{\sum_{v \in \gamma} V|A \rightarrow C| * V|C \rightarrow B|}{V|A \rightarrow C|}$$

γ is a group of recommenders.

$V|A \rightarrow C|$ is trust vector of node A to C.

$V|C \rightarrow B|$ is trust vector of node C to B.

Probability that data packets received can be defined by,

$$P_B^A = (1-p_{A,B}) * (1-p_{B,A})$$

$p_{A,B}$ is packet loss probability from node A to node B, while ,
 $p_{B,A}$ is packet loss probability from node B to node A.

For any node n_k , if $DS_k < DS_{min}$, where DS_{min} is the minimum threshold value, its trust vector value is further decremented as

$$Tv_i = Tv_i - \alpha_2 \tag{5}$$

For all the other nodes with $DS_k > DS_{min}$, the trust counter values are further incremented as

$$Tv_i = Tv_i + \alpha_2 \tag{6}$$

Where α_2 is another step value with $\alpha_2 < \alpha_1$.

For a node n_k , if $Tv_k < Tv_{thr}$, where Tv_{thr} is the trust threshold vector value, then that node is considered and marked as malicious. If the source does not get the RREP packet or RERR packet for a time period of t seconds, it will be considered as a node failure or link failure. Then the route discovery process is initiated by the source again. The same procedure is repeated for the other routes R2, R3 etc and either a route without a malicious node or with least number of malicious node, is selected as the reliable route.

IV. SIMULATION DIAGRAM& RESULTS

Ta are the auxiliary switch and its driving signal, which is generated by the PWM. Co , Vo , Io , and Ro describe the output capacitor, voltage, current, and equivalent load, respectively. It provides tools to create and edit fuzzy inference systems. Allows integrating fuzzy system into simulation with Simulink. It is possible to create stand alone C programs that call fuzzy system built with MATLAB. The tool box provides three categories of tools. They are as follows

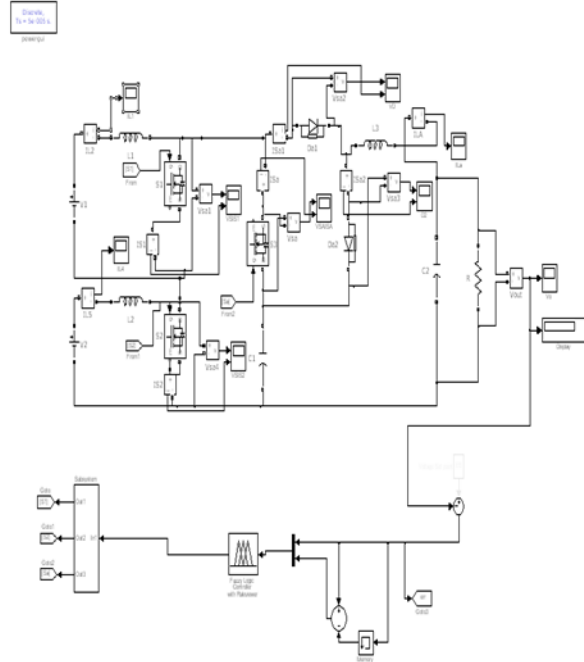


Figure 3 Simulation Diagram with using FLC

- i) Command line functions
- ii) Graphical or Interactive tools
- iii) Simulink blocks

The main difficulty in the mathematical analysis of fuzzy models is that they are inherently nonlinear and, therefore, classical control theory with its emphasis on linear systems is difficult to apply or cannot be applied at all. Multiple-input and single-output rule-based system considered in it. A membership function associated with a given fuzzy set maps an input value to its appropriate membership. Fuzzy systems theory enables us to utilize qualitative, linguistic information about a system to construct a mathematical model for it.

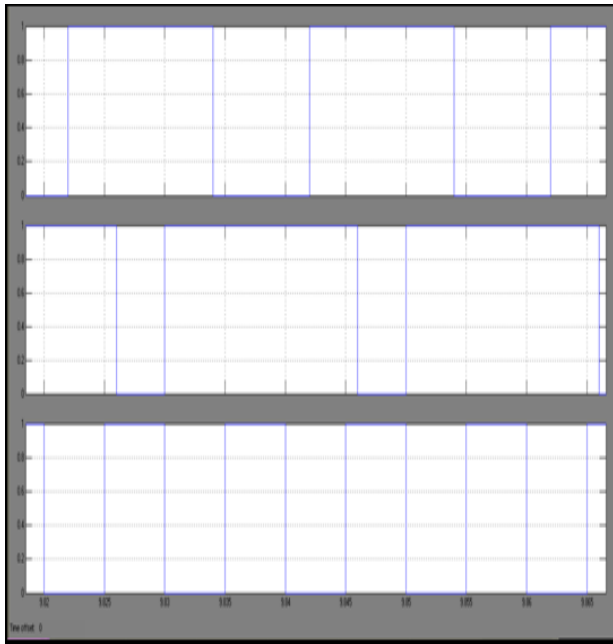


Figure 4. Triggering Pulse For S₁, S₂, S₃

For many real-life systems, which are highly complex and inherently nonlinear, conventional approaches to modeling are not easy to apply, whereas the fuzzy approach might be a very helpful alternative. The collection of rules is called the rule base. The rules are in “IF THEN” format and formally the IF side conditions.

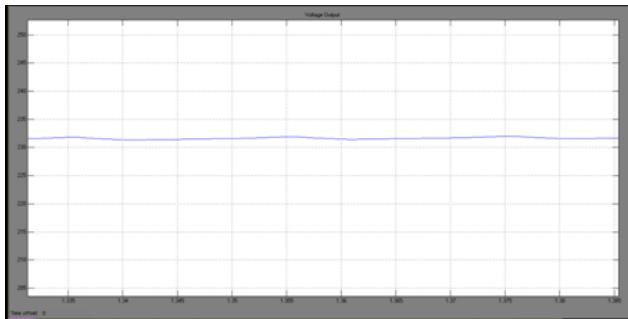


Figure 5 Output Voltage Without Controller

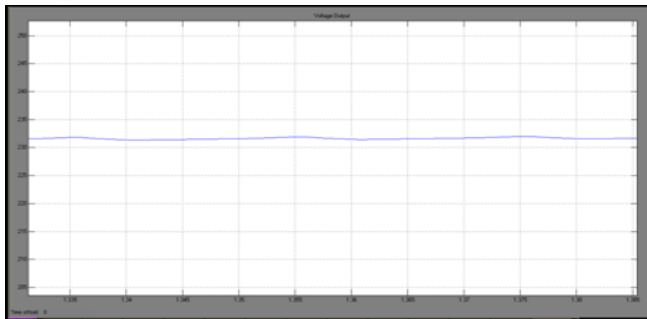


Figure 6 Voltage Waveform For FLC

From the figure 5 and figure 6, the output voltage waveform, both the single and dual power supply state under

FLC efficiency is approximately 95%, that means it is a “stable dc output”.

V. MODEL CALCULATION

FOR DUAL SUPPLY WITHOUT FEEDBACK

$$\text{Efficiency}_2 = \text{Output power} / \text{Input Power}$$

$$= (1.9 * 10^3) / (2.2 * 10^3) = 86.3\%$$

$$\text{Efficiency}_1 = \text{Output power} / \text{Input Power}$$

$$= (2 * (10^3)) / (2.2 * 10^3) = 90.9\%$$

$$\text{Efficiency}_2 / \text{Efficiency}_1 = 86.3 / 90.9 = 94.93\%$$

FOR DUAL SUPPLY WITH FLC

$$\text{Efficiency}_2 = \text{Output power} / \text{Input Power}$$

$$= (1.94 * 10^3) / (2.2 * 10^3) = 88.18\%$$

$$\text{Efficiency}_1 = \text{Output power} / \text{Input Power}$$

$$= (2 * (10^3)) / (2.2 * 10^3) = 90.9\%$$

$$\text{Efficiency}_2 / \text{Efficiency}_1 = 88.18 / 90.9 = 97\%$$

VI. CONCLUSION

This study has successfully developed a ZVS dual-input converter with hybrid power. In the dual power-supply state, the conduction loss can be effectively reduced by topological design of series connection of two input circuits. Besides, the reverse-recovery currents of the diodes are slight as well as the switching losses of the switches are effectively reduced. The maximum efficiency of the proposed converter operated in both operational states is higher than 95%. If the proposed ZVS dual-input converter in this study is used for non-isolated PV applications, the ground leakage current issue due to the high-frequency voltage swing occurs which could be solved by the adoption of an EMI filter for a dc power supply application or the integration with advanced inverter topologies for an ac-module application in the future research.

REFERENCES

- [1]. S. Al-Hallaj, “More than enviro-friendly: Renewable energy is also good for the bottom line,” IEEE Power Energy Mag., vol. 2, no. 3, pp. 16–22, May/Jun. 2004.
- [2]. P. Fairley, “The greening of GE,” IEEE Spectrum, vol. 42, no. 7, pp. 28–33, Jul. 2005.
- [3]. R. C. Dugan, T. S. Key, and G. J. Ball, “Distributed resources standards,” IEEE Ind. Appl. Mag., vol. 12, no. 1, pp. 27–34, Jan./Feb. 2006.
- [4]. B. Yang, W. Li, Y. Zhao, and X. He, “Design and analysis of a grid connected photovoltaic power system,” IEEE Trans. Power Electron., vol. 25, no. 4, pp. 992–1000, Apr. 2010.
- [5]. S. K. Kim, J. H. Jeon, C. H. Cho, J. B. Ahn, and S. H. Kwon, “Dynamic modeling and control of a grid-connected hybrid generation system with versatile power transfer,” IEEE Trans. Ind. Electron., vol. 55, no. 4, pp. 1677–1688,

Apr. 2008.

- [6]. M. B. Camara, H. Gualous, F. Gustin, and A. Berthon, "Design and newcontrol of DC/DC converter to share energy between super capacitors and batteries in hybrid vehicles," IEEE Trans. Veh. Technol., vol. 57, no. 5,pp. 2721–2735, Sep. 2008.
- [7]. T. Bhattacharya, V. S. Giri, K. Mathew, and L. Umanand, "Multiphase bidirectional flyback converter topology for hybrid electric vehicles,"IEEE Trans. Ind. Electron., vol. 56, no. 1, pp. 78–84, Jan. 2009.
- [8]. S. H. Park, S. R. Park, J. S. Yu, Y. C. Jung, and C. Y. Won, "Analysis and design of a soft-switching boost converter with an HI-bridge auxiliary resonant circuit," IEEE Trans. Power Electron., vol. 25, no. 8,pp. 2142–2149, Aug. 2010.
- [9]. Y. C. Liu and Y. M. Chen, "A systematic approach to synthesizing multiinput DC–DC converters," IEEE Trans. Power Electron., vol. 24, no. 1,pp. 116–127, Jan. 2009.
- [10]. Y. M. Chen, Y. C. Liu, S. C. Hung, and C. S. Cheng, "Multi-input inverte for grid-connected hybrid PV/wind power system," IEEE Trans. Power Electron., vol. 22, no. 3, pp. 1070–1077, May 2007.
- [11]. R. J. Wai, C. Y. Lin, L. W. Liu, and Y. R. Chang, "High-efficiency singlestage bidirectional converter with multi-input power sources," Inst. Electr. Eng. Proc.: Electr. Power Appl., vol. 1, no. 5, pp. 763–777, Sep. 2007.
- [12]. R. J.Wai, C. Y. Lin, and Y. R. Chang, "High step-up bidirectional isolated converter with two input power sources," IEEE Trans. Ind. Electron.,vol. 56, no. 7, pp. 2629–2643, Jul. 2009.
- [13]. H. Tao, J. L. Duarte, andM. A.M. Hendrix, "Three-porttriple-halfbridgebidirectional converter with zero voltage switching," IEEE Trans. Power Electron., vol. 23, no. 2, pp. 782–792, Mar. 2008.
- [14]. H. Matsuo, W. Z. Lin, F. Kurokawa, T. Shigemizu, and N. Watanabe, "Characteristics of the multiple-input DC–DC converter," IEEE Trans.Ind. Electron., vol. 51, no. 3, pp. 625–631, Jun. 2004.
- [15]. M. Marchesoni and C. Vacca, "New DC–DC converter for energy storagesystem interfacing in fuel cell hybrid electric vehicles," IEEE Trans.Power Electron., vol. 22, no. 1, pp. 301–308, Jan. 2007.

and**M.E.** in electrical and electronics engineering (Power Electronics and Drives) in AlagappaChettiar College of Engineering and Technology, Karaikudi, India, in 2007. Her research interest includes Boost converters, Neural Networks and fuzzy logic, Dc-dc converters.

Authors Profile



M.MuthuKumaran received the **B.E.** degree in electrical and electronics engineering from the sree sowdambika college of engineering affiliated to Anna University, Chennai, India, in 2010. Currently doing **M.E.** degree electrical and electronics engineering (Power Electronics and Drives) in SethuInstutue Of Technology, Kariapatti, India. His research interest includes Boost converters, Neural Networks and fuzzy logic, Dc-dc converters



K.Radha Lakshmi received the **B.E.** degree in electrical and electronics engineering from the Syed Ammal Engineering college, Ramanathapuram, Anna University, Chennai, India, in 2002.